

Synthesis of Hierarchical FeWO₄ Architectures with {100}-Faceted Nanosheet Assemblies as a Robust Biomimetic Catalyst

Tian Tian,[†] Lunhong Ai,^{*,†} Xiaomin Liu,[†] Lili Li,[†] Jie Li,[‡] and Jing Jiang^{*,†}

[†]Chemical Synthesis and Pollution Control Key Laboratory of Sichuan Province, College of Chemistry and Chemical Engineering, China West Normal University, Nanchong 637002, People's Republic of China

[‡]Institute of Nanoscience and Nanotechnology, College of Physical Science and Technology, Central China Normal University, Wuhan 430079, People's Republic of China

Supporting Information

ABSTRACT: Surface structure is of special significance to the heterogeneous catalysis, because catalysis is primarily a surface phenomenon. Therefore, a comprehensive understanding of the relationship between the catalytic activity and surface structure is of great importance. Herein, hierarchical FeWO₄ architectures assembled by {100}-faceted nanosheets have been successfully synthesized by a facile one-pot solvothermal method and employed as a novel biomimetic catalyst mimicking enzyme for the first time. Due to the large density of terminal iron atoms per unit surface area on the {100} facet, the FeWO₄ architectures exhibited excellent peroxidase-like activity for the catalytic oxidation of peroxidase substrate 3,3',5,5'-tetramethylbenzidine (TMB) to produce a blue color reaction in the presence of H₂O₂. Using the FeWO₄ architectures as peroxidase mimetics, a colorimetric sensor for H₂O₂ was developed, which provided good response toward H₂O₂ concentration over a range from 0.95 to 66.7 μM with a detection limit of 0.28 μM. The proposed colorimetric method can be further extended for the sensitive detection of glucose by coupling with glucose oxidase (GOx). The limit of detection for glucose was determined to be as low as 0.67 μM and the linear range was from 4 to 60 μM. It is believed that these findings are useful in understanding the peroxidase-like activity of catalysts with facet exposure and suggest a new strategy to pursue for highly active peroxidase-like catalysts.

1. INTRODUCTION

Surface properties are of pivotal importance in various chemical processes, because the physicochemical properties of solid materials closely depend on the surface-related atomic, electronic and geometric structures.^{1–4} Recently, considerable attention has been given to the design and manipulation of a well-defined structure with a specific facet exposure,^{5–9} which provides a critical way to finely tailor the physicochemical properties and thus rationally optimizes their reactivity and selectivity. As such, surface structure control is of special significance to the heterogeneous catalysis, because a heterogeneous catalytic reaction involves many surface-related steps, such as adsorption and activation of reactants on specific surface sites, chemical transformation of adsorbed species and desorption of products.^{10–12} For example, Lu and co-workers realized the synthesis of anatase TiO₂ with highly reactive {001} facets, which have paved a new way for the enhancement of photocatalytic performance.¹³ Huang et al. demonstrated that crystal-plane engineering of Cu₂O crystals could control the selective catalysis of propylene oxidation with molecular oxygen.¹⁴ The highly concave Pt nanoframes enclosed by {740} facets exhibited a higher electrocatalytic activity and improved long-term stability compared to the commercial Pt/C catalyst.¹⁵ Fe₂O₃ nanorods predominantly exposing {110} facets revealed high activity in heterogeneous photo-Fenton catalysis, which were more reactive than the basic {012} and {001} facets.¹⁶ We also found the facet-dependent photoreactivity and internal electric field orientation of BiOCl nanosheets arisen from the surface atomic structure.¹⁷ To this end, it is expected that facet

engineering would provide an exciting direction to pursue for highly active catalysts.

Recently, numerous efforts have been made in the design and construction of artificial enzymes that can imitate the essential and general principles of natural enzymes to overcome the limitations of natural enzymes.^{18–20} As highly stable and low-cost alternatives to natural enzymes, the functional inorganic nanomaterials including metals, oxides, sulfides and carbons have been proven to possess the unexpected peroxidase-like catalytic activity and have promising potential applications in bioanalytical and clinical chemistry.¹⁸ Despite these advances, there is still a great challenge to exploit a reliable strategy for the improvement and manipulation of peroxidase-like performance, because the present popular strategy mainly focuses on composition design of enzyme mimics. Most recently, Zhu and co-workers have observed the facet-dependent peroxidase-like activity in the catalytic system of Fe₃O₄ nanocrystals.²¹ The peroxidase-like activities of Fe₃O₄ nanocrystals followed the order of cluster spheres > triangular plates > octahedral, which were closely related to their preferential exposure of catalytically active crystal planes. Our group has also observed that the facet effect existed in peroxidase-like catalysis of the {001}-faceted BiOBr nanosheet microspheres.²² We inferred that the surface atomic structure of {001} facet in BiOBr nanosheet microspheres was favorable for the generation of oxygen

Received: October 18, 2014

Revised: January 14, 2015

Accepted: January 14, 2015

Published: January 26, 2015



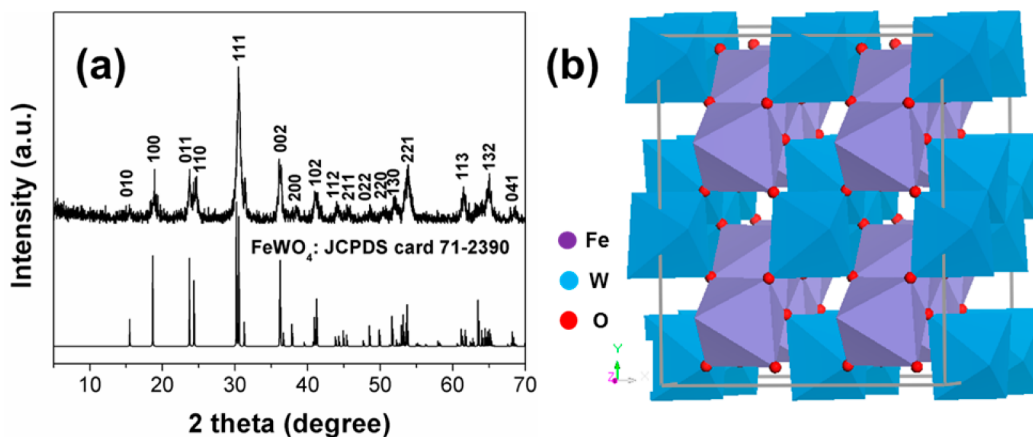


Figure 1. (a) XRD pattern of the FeWO₄ architectures and (b) crystal structure of FeWO₄.

vacancies to promote the peroxidase-like reaction. Therefore, it is postulated that facet control should be an effective strategy for the rational design and fabrication of high performance peroxidase-like catalysts. However, studies on the synthesis of enzyme mimics with facet exposure are still rather sparse.^{21–23}

Glucose is not only the main source of energy for the body but also the product in a wide range of reactions catalyzed by a large number of oxidases, which plays an important role in clinical diagnostics, biotechnology, environmental pollution control and food industries.^{24,25} Therefore, the development of a simple and reliable sensor for the accurate determination of glucose levels is of immense scientific technological significance. In the present study, we report the successful synthesis of the hierarchical FeWO₄ architectures assembled from {100}-faceted nanosheets via a facile and reproducible solvothermal process, and demonstrate their remarkably intrinsic peroxidase-like catalytic activity for the first time. Furthermore, the FeWO₄ architectures as a robust peroxidase mimic provide the simple and sensitive colorimetric assays. Compared with the previously reported nanostructured peroxidase mimics, the FeWO₄ architectures manifest a high sensitivity and low detection limit for the optical detection of H₂O₂ and glucose.

2. EXPERIMENTAL SECTION

2.1. Materials. FeCl₃·6H₂O, Na₂WO₄, sodium acetate (NaAc), ethylene glycol (EG), acetic acid (HAc) and H₂O₂ (30 wt %) were purchased from Kelong Chemical Reagents company (Chengdu, China). Na₂HPO₄, NaH₂PO₄ and 3,3'5,5'-tetramethylbenzidine (TMB) were purchased from Aladin Ltd. (Shanghai, China). Glucose, fructose, lactose, maltose and glucose oxidase (GOx, 340 U·mg⁻¹) were purchased from Sangon Biochemical Engineering Technology Co., Ltd. (Shanghai, China). All chemicals used in this study were of analytical grade and used without further purification.

2.2. Synthesis of the FeWO₄ Architectures. Hierarchical FeWO₄ architectures were prepared based on a previous method with some modification.²⁶ In a typical procedure, 3 mL of aqueous FeCl₃·6H₂O solution (0.33 M) was added to 3 mL of aqueous Na₂WO₄·2H₂O (0.33 M) solution under magnetic stirring, followed by the addition of NaAc (10 mmol). Then, 14 mL of ethylene glycol was added, and the solution was vigorously stirred for 30 min. The solution was transferred to a 50 mL Teflon-lined autoclave that was sealed and heated at 200 °C for 12 h. The as-prepared product was centrifuged at 6000

rpm and washed with absolute ethanol and distilled water several times, and then dried at 60 °C for 12 h in air.

2.3. Characterization. The powder X-ray diffraction (XRD) measurements were recorded on a RigakuDmax/Ultima IV diffractometer with monochromatized Cu K α radiation ($\lambda = 0.154\text{18 nm}$). The morphology was observed with scanning electron microscopy (SEM, JEOL 6700-F) and transmission electron microscopy (TEM, FEI Tecnai G20). The elemental compositions of the samples were characterized by energy-dispersive X-ray spectroscopy (EDS, Oxford instruments X-Max). X-ray photoelectron spectroscopy (XPS) measurements were recorded on a PerkinElmer PHI 5000C spectrometer using monochromatized Al K α excitation. All binding energies were calibrated by using the contaminant carbon (C_{1s} = 284.6 eV) as a reference.

2.4. Bioassay. The peroxidase-like activity of the FeWO₄ architectures was tested by the catalytic oxidation of the peroxidase substrate TMB in the presence of H₂O₂. The kinetic measurements were carried out in time course mode by monitoring the absorbance change at 652 nm. The assays were carried out by varying concentrations of TMB at a fixed concentration of H₂O₂ or vice versa. Experiments were performed using 38 $\mu\text{g}\cdot\text{mL}^{-1}$ FeWO₄ in 1600 μL of reaction buffer (0.2 M NaAc, pH 3.0) with 0.198 mM TMB as the substrate, or 4.76 mM H₂O₂ as the substrate, unless otherwise stated. The apparent kinetic parameters were calculated using Lineweaver-Burk plots of the double reciprocal of the Michaelis-Menten equation: $1/v = K_m/V_{\max}(1/[S] + 1/K_m)$, where v is the initial velocity, V_{\max} is the maximal reaction velocity, $[S]$ is the concentration of substrate and K_m is the Michaelis constant.

2.5. H₂O₂ Detection Using the FeWO₄ Architectures as Peroxidase Mimetic. In a typical experiment, 80 μL of FeWO₄ dispersion (1 $\text{mg}\cdot\text{mL}^{-1}$) was mixed in 1600 μL of NaAc buffer solution (0.2 M NaAc, pH 3.0), followed by adding 400 μL of TMB solution (1 mM, ethanol solution). Then, 20 μL of H₂O₂ with different concentrations was added into the mixture. The mixed solution was incubated at 40 °C for 30 min.

2.6. Glucose Detection Using the FeWO₄ Architectures and Glucose Oxidase (GOx). Glucose detection was carried out as follows: first, 100 μL of GOx aqueous solution (1 $\text{mg}\cdot\text{mL}^{-1}$) and 100 μL of glucose with different concentrations were mixed in 500 μL of phosphate buffer (PBS, pH 7.0) and incubated at 37 °C for 1 h; then 200 μL of TMB (10 mM,

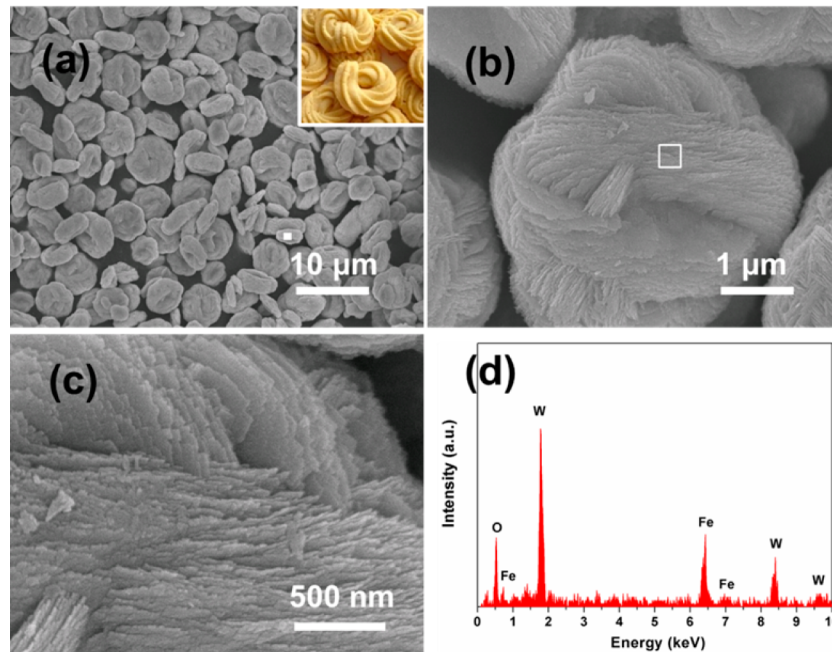


Figure 2. SEM images (a–c) and EDS spectrum (d) of the FeWO_4 architectures. Inset in panel a is a photo of cookies.

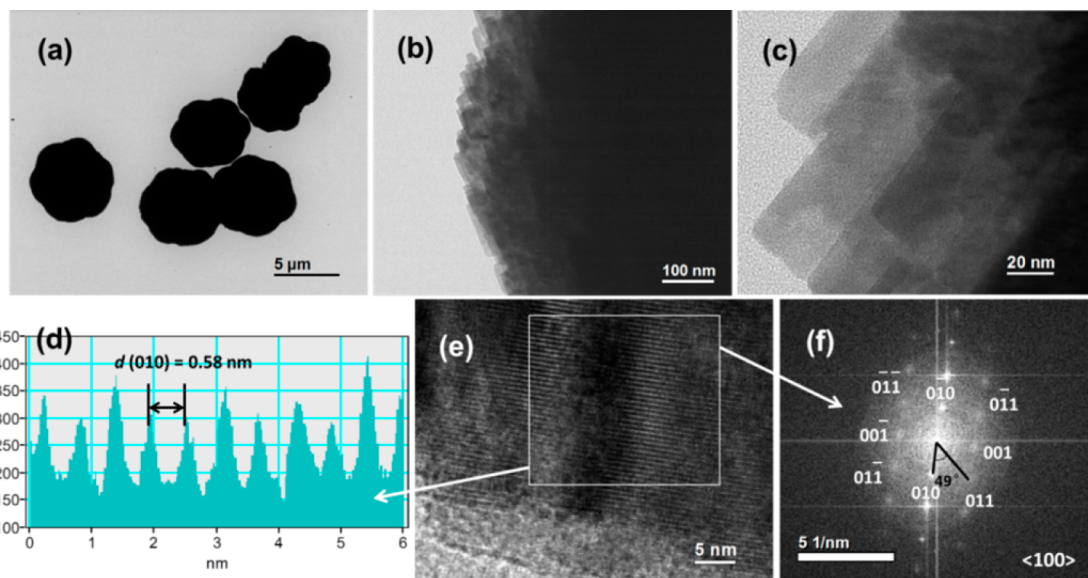


Figure 3. TEM (a–c), HRTEM images (e), corresponding line profile (d) and FFT pattern (f) of the FeWO_4 architectures.

ethanol solution), 100 μL of the FeWO_4 stock solution (2 mg· mL^{-1}) and 4 mL of NaAc buffer (0.2 M, pH 3.0) were successively added to the glucose reaction solution; finally, the mixed solution was incubated at 40 °C for 30 min for standard curve measurement.

3. RESULTS AND DISCUSSION

Figure 1a shows a typical powder X-ray diffraction (XRD) pattern of the as-synthesized FeWO_4 architectures. All of the diffraction peaks agree very well with the standard data (JCPDS file no. 71-2390) of monoclinic phase of FeWO_4 with a space group of $P\bar{2}c$ (13) and lattice parameters of $a = 4.753 \text{ \AA}$, $b = 5.720 \text{ \AA}$, $c = 4.968 \text{ \AA}$ and $\beta = 90.8^\circ$. No other additional peaks are detected from XRD pattern, indicating the high purity of the FeWO_4 architectures. The well-defined peak reveals the

good crystallinity of the FeWO_4 architectures. Figure 1b schematically illustrates the crystal cell structure of FeWO_4 , presenting a wolframite-type monoclinic structure. Both Fe and W atoms are coordinated to six oxygen atoms, forming octahedral $[\text{FeO}_6]/[\text{WO}_6]$ clusters.

Figure 2a–c shows the typical scanning electron microscopy (SEM) images of the FeWO_4 products at different magnifications. As shown in Figure 2a, the FeWO_4 products are almost entirely composed of a large quantity of nearly monodispersed cookies-like microstructures with uniform round hexangular shape. The diameters and thicknesses of these round hexangular architectures are estimated to be about 4–6 μm and 1.2–2.0 μm , respectively. A higher magnification image (Figure 2b) exhibits the detailed front surface information on such an architecture. It can be seen that these round hexangular

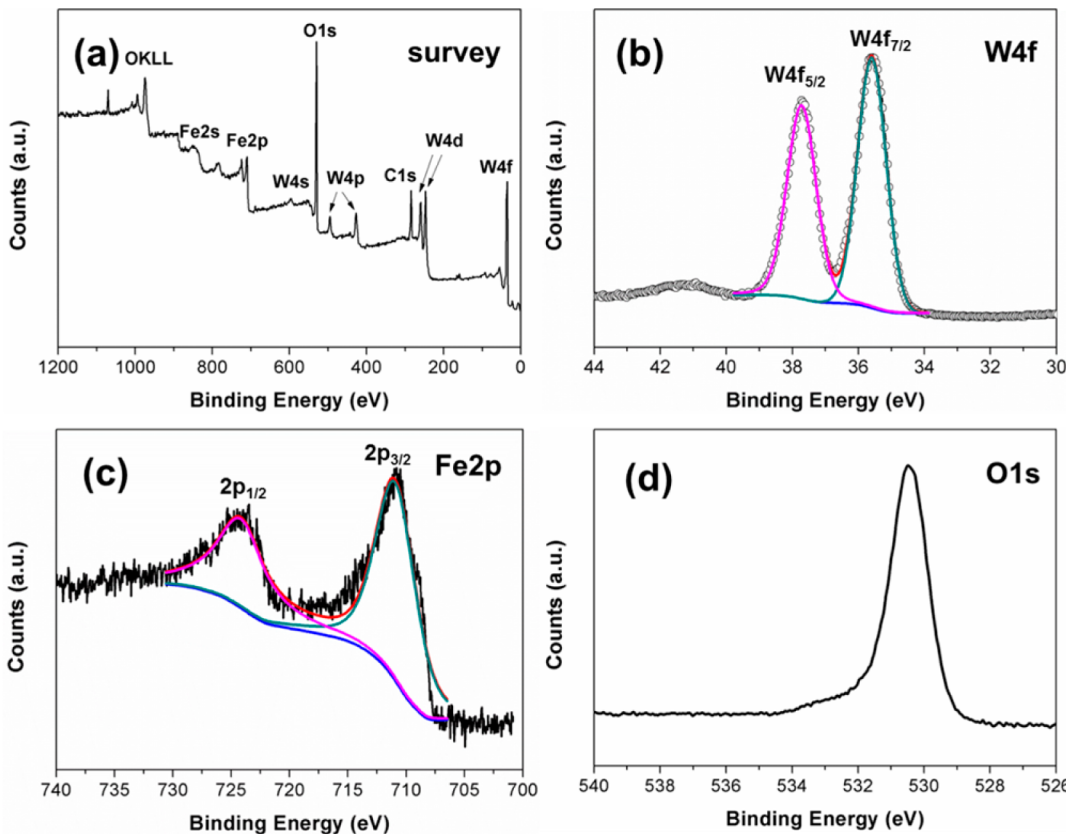


Figure 4. XPS spectra of the FeWO_4 architectures: survey (a), W 4f (b), Fe 2p (c) and O 1s (d).

architectures are actually built from a large number of two-dimensional thin nanosheets with an average thickness of 20 nm. The nanosheets are densely aligned and intercrossed with each other to form the unique multilayer stacked structures, as disclosed by Figure 2c. The X-ray energy dispersive spectroscopy (EDS) spectrum (Figure 2d) of the selected area in Figure 2b reveals that the FeWO_4 architectures mainly contain Fe, W and O elements with desirable stoichiometry. The quantitatively calculated surface mole ratio of Fe to W in the FeWO_4 architectures is approximately 1.06:1, agreeing with its feeding ratio (1:1).

To gain the detailed information about the structure feature of the products, the FeWO_4 architectures were further characterized by transmission electron microscopy (TEM). Figure 3a presents representative TEM image of the FeWO_4 architectures. It confirms that the hexangular microstructures are composed of six nearly equal petals, which looks like a hexangular symmetrically extended flower as a whole. The hexangular architectures have an average diameter of about 5.5 μm . The dark color of the each hexangular architecture indicates the compact structure feature, consistent with above SEM observations. The TEM image (Figure 3b) of individual hexangular architecture further depicts the closely packed structures, where a clear contrast between the central and fringe part can be clearly seen. A higher magnification TEM image (Figure 3c) reveals that the hexangular architectures are indeed constructed with stacks of ultrathin nanosheets. A high resolution (HR)TEM image (Figure 3e) recorded from the individual nanosheet side displays that the lattice fringes are a spacing of 0.58 nm (see the line profile in Figure 3d), corresponding to the lattice spacing of the (010) planes. The corresponding fast Fourier transform (FFT) pattern (Figure 3f)

can be indexed into diffraction spots of the [100] zone axis. The angle between {010} and {011} of 49° agrees well with the theoretical value (see the Supporting Information). These results indicate that the nanosheets are highly crystalline and enclosed by dominant {100} facets (Supporting Information, Figure S1).

The chemical composition and chemical states of the FeWO_4 architectures were further determined by X-ray photoelectron spectroscopy (XPS). The binding energies in the spectrum were calibrated using the contaminant carbon ($\text{C}_{1s} = 284.6$ eV) as a reference. The survey spectrum shown in Figure 4a reveals the products are composed of Fe, W and O elements. Figure 4b presents the high resolution XPS spectrum of W 4f. The two peaks at 37.7 and 35.6 eV are assigned to $\text{W } 4f_{5/2}$ and $\text{W } 4f_{7/2}$, respectively, suggesting that W exists in the chemical state of W^{6+} .²⁷ The high resolution XPS spectrum of Fe 2p shown in Figure 4c presents two peaks at 724.4 and 711.1 eV, corresponding to $\text{Fe } 2p_{3/2}$ and $\text{Fe } 2p_{1/2}$, respectively, in good agreement with the values of Fe^{2+} .²⁸ The asymmetric peak at 530.4 eV (Figure 4d) is representative of the O 1s binding energy for lattice O^{2-} . The quantitative analysis shows that the atom ratio of W/Fe is about 1:1.01.

The peroxidase-like activity of the FeWO_4 architectures was evaluated by the catalytic oxidation of a typical peroxidase substrate 3,3',5,5'-tetramethylbenzidine (TMB). This reaction could produce a blue color in the presence of H_2O_2 , which can be easily monitored by the UV-vis absorbance spectroscopy. Figure 5A shows the UV-vis spectra of TMB solutions in acetate buffer (pH 3.0) under different conditions. It is clear that neither the H_2O_2 (curve b) nor the FeWO_4 architectures (curve c) is unable to induce a significant color change of the TMB solution (curve a). In contrast, upon the addition of the

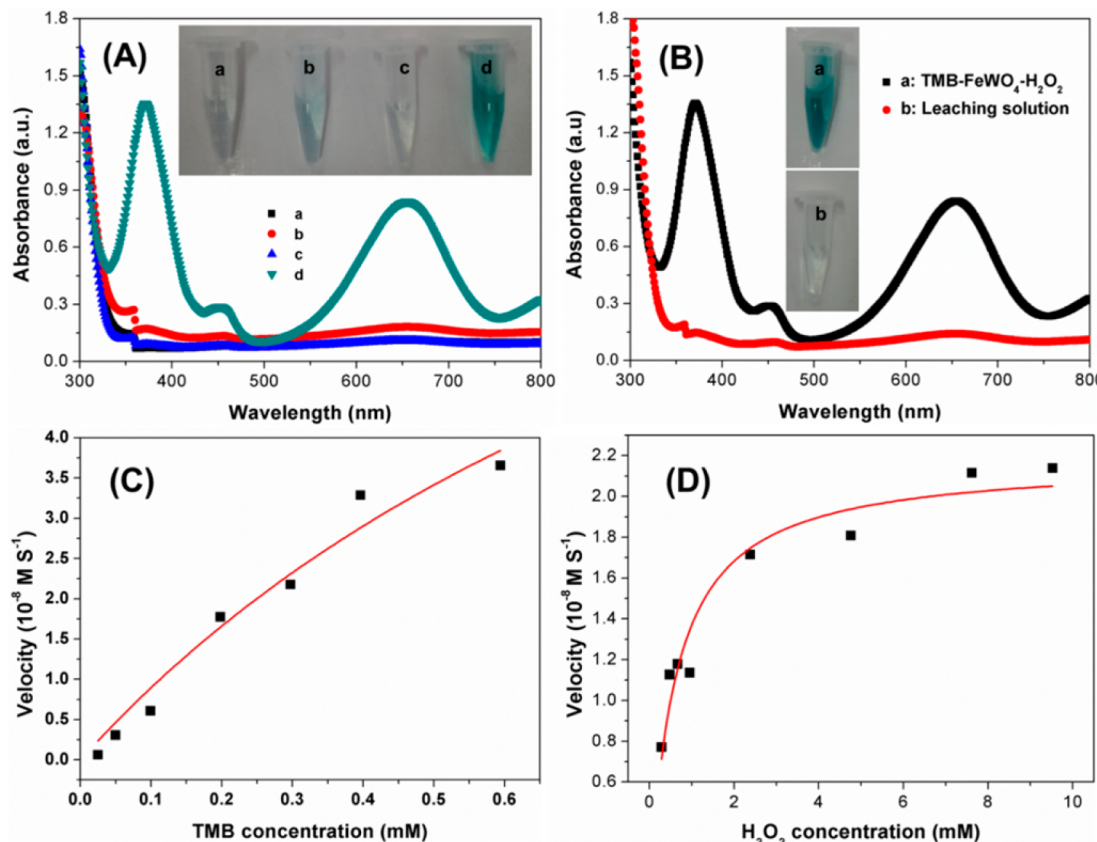


Figure 5. (A) UV-vis spectra and corresponding photographs (inset) of different reaction systems: TMB solution (a), H₂O₂-TMB (b), FeWO₄-TMB (c) and H₂O₂-FeWO₄-TMB (d) in acetate buffer (pH 3.0). ([TMB], 0.19 mM; [H₂O₂], 370 mM; [FeWO₄], 38 μ g·mL⁻¹) at 40 °C. (B) UV-vis spectra of the H₂O₂-TMB system in the presence of the leaching solution. (C, D) Steady-state kinetic assay of the FeWO₄ architectures. The concentration of H₂O₂ was 4.76 mM and the TMB concentration was varied. The concentration of TMB was 0.198 mM and the H₂O₂ concentration was varied.

FeWO₄ architectures, the TMB-H₂O₂ solution exhibits a deep blue color with an intense characteristic absorbance at 369 and 652 nm, which are ascribed to the charge-transfer complexes derived from the one-electron oxidation of TMB.^{29,30} These results suggest that the FeWO₄ architectures indeed possess the remarkably catalytic activity toward the oxidation of TMB substrate in the presence of H₂O₂. The peroxidase-like activity of the FeWO₄ architectures was further confirmed by catalytic oxidation of the other peroxidase substrate *o*-phenylenediamine (OPD) with H₂O₂, which could also produce a typical color change (Supporting Information, Figure S2). Note that the leaching solution from the catalysts possibly confuses the observed catalytic activity. It is necessary to rule out the possibility that the observed catalytic activity results from the FeWO₄ itself rather than from the free leaching ions. As shown in Figure 5B, the leaching solution exhibits the negligible activity, evidenced by the colorless reaction solution, which confirms that the observed peroxidase-like activity is indeed originated from the intact FeWO₄. Moreover, the crystal structure of the FeWO₄ architectures remains unchanged after the catalytic reaction (Supporting Information, Figure S3). These observations clearly suggest that the FeWO₄ architectures possess an intrinsic peroxidase-like activity. It should be mentioned that Fe-containing composition is an important factor to determine the peroxidase-like catalytic activity of the Fe-based nanomaterials. The iron atoms generally act as the active sites to produce reactive ·OH species in the Fe-based nanomaterials for peroxidase-like catalysis (Fe²⁺ + H₂O₂ →

Fe³⁺ + ·OH + OH⁻; ·OH + TMB → oxTMB).^{30–34} As widely accepted, iron oxides like typical Fe₂O₃ and Fe₃O₄ have been demonstrated as highly active peroxidase mimetics. As a comparison, we conducted the TMB oxidation with the nanosturctured Fe₂O₃ and Fe₃O₄ in the presence of H₂O₂. We found the peroxidase-like catalytic activity of the FeWO₄ architectures was much higher than that of Fe₂O₃ and Fe₃O₄ (Supporting Information, Figure S4), demonstrating the high performance of Fe-based FeWO₄ in peroxidase-like catalysis. More significantly, under identical conditions, the FeWO₄ architectures also show the better peroxidase-like catalytic activity than that of the FeWO₄ microcrystals without specific surface exposure (Supporting Information, Figure S4), most probably due to the presence of exposed highly active {100} facets.

Similar to other peroxidase mimics and horse radish peroxidase (HRP), the catalytic activity of the FeWO₄ architectures relies on various operation parameters, such as solution pH, reaction temperature and H₂O₂ concentration. A series of catalytic reaction were conducted by varying the pH from 2.0 to 10.0, the temperature from 20 to 80 °C, and the H₂O₂ concentration from 0.95 to 545 μ M. As shown in Figure S5 (Supporting Information), the catalytic reaction requires the suitable pH and temperature, due to the instability of H₂O₂ at high pH and temperature. The optimal conditions are approximately pH 3.0 and 40 °C, and 4.8 mM H₂O₂, similar to those previously reported for nanostructure-based peroxidase mimetics and HRP.^{35,36}

To gain insight into the peroxidase-like catalytic activity of the FeWO_4 architectures, we further carried out the steady-state kinetic assays by changing one substrate concentration while keeping the other substrate concentration constant. As shown in Figure 5C,D, the curves display a typical Michaelis–Menten behavior in a specific range of substrate concentrations. By plotting initial velocities against substrate concentrations, the kinetic parameters including maximum initial velocity (V_{\max}) and Michaelis–Menten constant (K_m) can be determined using Michaelis–Menten equation.³⁷ Generally, K_m characterizes binding affinity of the enzyme to the substrates and the lower K_m value implies the stronger affinity. The K_m value of the FeWO_4 architectures for the H_2O_2 substrate is found to be 0.59 mM, much lower than the reported values of HRP and other nanomaterials-based peroxidase mimics (Supporting Information, Tables S1 and S2), indicating that the FeWO_4 architectures have a higher affinity toward H_2O_2 than HRP and other mimics. In addition, the K_m value of the FeWO_4 architectures for the TMB substrate is larger than that of HRP, suggesting that the FeWO_4 architectures have a lower affinity for TMB than HRP. This phenomenon is consistent with previous observations on other nanomaterial-based peroxidase mimics.^{38,39}

It is generally accepted that the reactivity of a catalyst is closely associated with its surface property, as a high density of surface unsaturated coordinated atoms endow it with a high surface energy of the crystal facet, which is favorable for heterogeneous reactions. Our recent studies have also demonstrated the enhanced catalytic activity of BiOX (X = Cl,¹⁷ Br²²) nanosheets arisen from the surface facet exposure. On the basis of the above results, we will discuss the high reactivity of the FeWO_4 architectures with {100}-faceted nanosheets. Figure 6 illustrates the atomic structure of

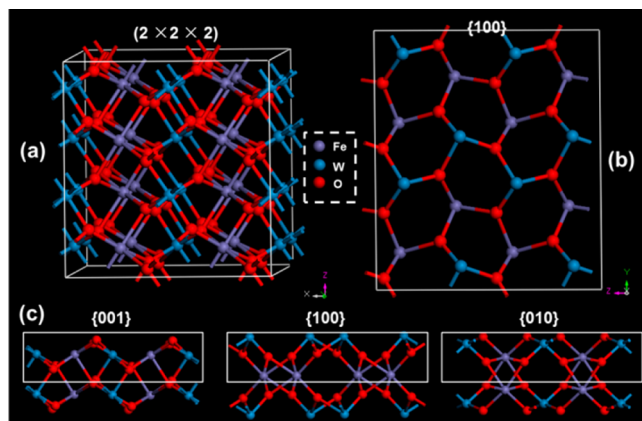


Figure 6. Structure model illustration of a monoclinic FeWO_4 crystal: (a) $(2 \times 2 \times 2)$ cell structure; (b) top view of {100} facets and (c) side view of {001}, {100} and {010} facets.

FeWO_4 . It is clear that the {100} facet contains a puckered 6^3 net along the plane, which has a higher atomic density than that of {001} and {010} facets containing the distorted quadrilateral net (Supporting Information, Figure S6). Note that iron atoms act as the active species for peroxidase-like catalysis ($\text{Fe}^{2+} + \text{H}_2\text{O}_2 \rightarrow \text{Fe}^{3+} + \cdot\text{OH} + \text{OH}^-$; $\cdot\text{OH} + \text{TMB} \rightarrow \text{oxTMB}$), which is critical to the catalytic performance of FeWO_4 . Naturally, the {100} facet with higher iron atom density should be much more reactive. For this consideration, the number density of iron atoms on different crystal facets is

calculated (Supporting Information, Table S3). The number of terminal iron atoms per unit surface area on the {100} facet is roughly two times as high as that found on the {001} facet and about 1.7 times that of {010} facet. Furthermore, we employ the well-established fluorescence method to determine $\cdot\text{OH}$ radicals in the catalytic system to confirm the reactivity of iron species toward H_2O_2 (Supporting Information, Figure S7). It is clear that the significant change in fluorescent intensity at 425 nm is observed for $\text{FeWO}_4-\text{H}_2\text{O}_2$ system, indicating the effective generation of $\cdot\text{OH}$ radicals. Noticeably, no observable fluorescent intensity is detected in the absence of the FeWO_4 . This solidly confirms that the FeWO_4 can catalytically activate H_2O_2 to produce $\cdot\text{OH}$ radicals that could react with TMB to produce the color reaction.

In light of the remarkably peroxidase-like activity of the FeWO_4 architectures, a simple colorimetric method was developed for the detection of H_2O_2 based on FeWO_4 -catalyzed color reaction. Figure 7a shows a typical H_2O_2

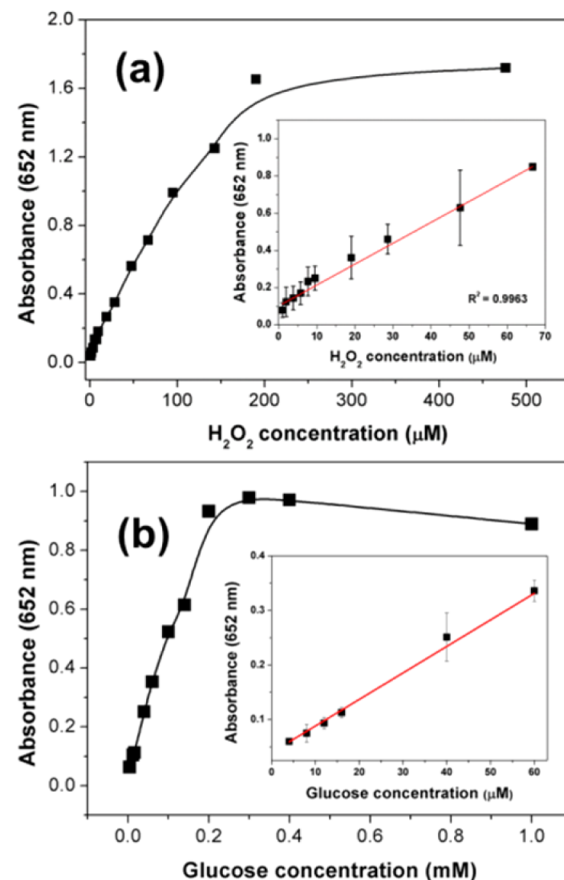


Figure 7. (a) Dose–response curve for H_2O_2 detection using the FeWO_4 architectures under the optimum conditions (inset: linear calibration plot for H_2O_2 detection). (b) Dose–response curve for glucose detection using the FeWO_4 architectures under the optimum conditions (inset: linear calibration plot for glucose detection).

concentration–response curve for the FeWO_4 architectures. H_2O_2 could be detected in a linear range from 0.95 to 66.7 μM ($R^2 = 0.9963$), and the limit of detection was 0.28 μM . Because GOx can specifically catalyze the glucose oxidation in the presence of oxygen to produce H_2O_2 , the proposed colorimetric method could be extended for the sensitive detection of glucose by coupling with GOx. Figure 7b shows a typical glucose concentration–response curve. Under optimum

conditions, a linear relationship was achieved between the absorbance and the glucose concentration in the range of 4 to 60 μM ($R^2 = 0.9961$), with a low detection limit of 0.67 μM , showing the higher sensitivity than those of the large number of oxides and faceted nanomaterials-based peroxidase mimics (Supporting Information, Table S2). To study the selectivity of the FeWO_4 -based colorimetric assay for glucose detection, control experiments were carried out using lactose, fructose and maltose instead of glucose, as shown in Figure S8 (Supporting Information). Even when the concentrations of glucose analogues are about 10-fold higher than that of glucose, the signals of glucose analogues are much lower than that of the glucose, and the color difference can be observed by the naked eye (Supporting Information, Figure S8). Thus, the colorimetric method developed here showed high sensitivity and selectivity toward glucose.

4. CONCLUSIONS

In summary, the FeWO_4 architectures assembled by {100}-faceted nanosheets have been prepared by a one-pot solvothermal method. The architectures show excellent intrinsic peroxidase-like catalytic activity due to the large density of terminal iron atoms per unit surface area on the {100} facet. Furthermore, the FeWO_4 architectures, as a robust peroxidase mimic, provided simple and sensitive colorimetric assays. Compared with the previously reported nanostructured peroxidase mimics, the FeWO_4 architectures manifest a high sensitivity and low detection limit for the optical detection of H_2O_2 and glucose. We believe this correlation between the catalytic activity and exposed facets will contribute to the rational design of peroxidase-like catalysts with high efficiency.

■ ASSOCIATED CONTENT

Supporting Information

Schematic illustration of the crystal orientation of the nanosheet, photographs and reaction schemes of the catalytic oxidation of TMB and OPD by the FeWO_4 architectures with H_2O_2 , XRD pattern of the FeWO_4 architectures after the catalytic reaction, UV-vis spectra of TMB- H_2O_2 reaction systems in the presence of different Fe-based catalysts, quantitative comparison of the catalytic activity of {100}-faceted FeWO_4 and FeWO_4 microcrystals (the measurements were performed in quintuplicate to reduce the error to as low as possible), SEM image of FeWO_4 microcrystals, effect of pH, temperature and H_2O_2 concentration on the peroxidase-like activity of the FeWO_4 architectures for the TMB oxidation, structure model illustration of a monoclinic FeWO_4 crystal, ·OH-trapping fluorescent spectra of FeWO_4 - H_2O_2 catalytic system, selectivity analysis for glucose detection by monitoring absorbance, comparison of the apparent Michaelis-Menten constant (K_m) and maximum reaction rate (V_m) of the FeWO_4 architectures and HRP, comparison of detection limit of H_2O_2 and glucose, and K_m value with H_2O_2 as the substrate of the FeWO_4 architectures and other reported nanomaterials-based mimics and density of exposed iron atoms on different planes of FeWO_4 crystal. This material is available free of charge via the Internet at <http://pubs.acs.org>.

■ AUTHOR INFORMATION

Corresponding Authors

*Lunhong Ai. E-mail: lhongai@cwnu.edu.cn, ah_ahong@163.com. Tel/Fax: +86-817-256808.

*Jing Jiang. E-mail: jjiang7659@cwnu.edu.cn, 0826zjjh@163.com. Tel/Fax: +86-817-256808.

Notes

The authors declare no competing financial interest.

■ ACKNOWLEDGMENTS

This work was supported by the National Natural Science Foundation of China (21207108 and 21103141), Sichuan Youth Science and Technology Foundation (2013JQ0012) and the Research Foundation of CWNU (12B018).

■ REFERENCES

- Zhou, Z.-Y.; Tian, N.; Li, J.-T.; Broadwell, I.; Sun, S.-G. Nanomaterials of High Surface Energy with Exceptional Properties in Catalysis and Energy Storage. *Chem. Soc. Rev.* **2011**, *40*, 4167.
- Liu, G.; Yu, J. C.; Lu, G. Q.; Cheng, H.-M. Crystal Facet Engineering of Semiconductor Photocatalysts: Motivations, Advances and Unique Properties. *Chem. Commun.* **2011**, *47*, 6763.
- Jing, L.; Zhou, W.; Tian, G.; Fu, H. Surface Tuning for Oxide-based Nanomaterials as Efficient Photocatalysts. *Chem. Soc. Rev.* **2013**, *42*, 9509.
- Huang, M. H.; Lin, P.-H. Shape-Controlled Synthesis of Polyhedral Nanocrystals and Their Facet-Dependent Properties. *Adv. Funct. Mater.* **2012**, *22*, 14.
- Han, X.; Jin, M.; Xie, S.; Kuang, Q.; Jiang, Z.; Jiang, Y.; Xie, Z.; Zheng, L. Synthesis of Tin Dioxide Octahedral Nanoparticles with Exposed High-Energy {221} Facets and Enhanced Gas-Sensing Properties. *Angew. Chem., Int. Ed.* **2009**, *48*, 9180.
- Yin, J.; Yu, Z.; Gao, F.; Wang, J.; Pang, H.; Lu, Q. Low-Symmetry Iron Oxide Nanocrystals Bound by High-Index Facets. *Angew. Chem., Int. Ed.* **2010**, *49*, 6238.
- Sun, H.; Ang, H. M.; Tadé, M. O.; Wang, S. Co_3O_4 Nanocrystals with Predominantly Exposed Facets: Synthesis, Environmental and Energy Applications. *J. Mater. Chem. A* **2013**, *1*, 14427.
- Yin, A.-X.; Min, X.-Q.; Zhang, Y.-W.; Yan, C.-H. Shape-Selective Synthesis and Facet-Dependent Enhanced Electrocatalytic Activity and Durability of Monodisperse Sub-10 nm Pt-Pd Tetrahedrons and Cubes. *J. Am. Chem. Soc.* **2011**, *133*, 3816.
- Long, R.; Mao, K.; Ye, X.; Yan, W.; Huang, Y.; Wang, J.; Fu, Y.; Wang, X.; Wu, X.; Xie, Y.; Xiong, Y. Surface Facet of Palladium Nanocrystals: A Key Parameter to the Activation of Molecular Oxygen for Organic Catalysis and Cancer Treatment. *J. Am. Chem. Soc.* **2013**, *135*, 3200.
- Zhou, K.; Li, Y. Catalysis Based on Nanocrystals with Well-Defined Facets. *Angew. Chem., Int. Ed.* **2012**, *51*, 602.
- Xie, X. W.; Li, Y.; Liu, Z. Q.; Haruta, M.; Shen, W. J. Low-Temperature Oxidation of CO Catalysed by Co_3O_4 Nanorods. *Nature* **2009**, *458*, 746.
- Suntivich, J.; May, K. J.; Gasteiger, H. A.; Goodenough, J. B.; Shao-Horn, Y. A. Perovskite Oxide Optimized for Oxygen Evolution Catalysis from Molecular Orbital Principles. *Science* **2011**, *334*, 1383.
- Yang, H. G.; Sun, C. H.; Qiao, S. Z.; Zou, J.; Liu, G.; Smith, S. C.; Cheng, H. M.; Lu, G. Q. Anatase TiO_2 Single Crystals with a Large Percentage of Reactive Facets. *Nature* **2008**, *453*, 638.
- Hua, Q.; Cao, T.; Gu, X.-K.; Lu, J.; Jiang, Z.; Pan, X.; Luo, L.; Li, W.-X.; Huang, W. Crystal-Plane-Controlled Selectivity of Cu_2O Catalysts in Propylene Oxidation with Molecular Oxygen. *Angew. Chem., Int. Ed.* **2014**, *53*, 4856.
- Xia, B. Y.; Wu, H. B.; Wang, X.; Lou, X. W. Highly Concave Platinum Nanoframes with High-Index Facets and Enhanced Electrocatalytic Properties. *Angew. Chem., Int. Ed.* **2013**, *52*, 12337.
- Zhou, X.; Lan, J.; Liu, G.; Deng, K.; Yang, Y.; Nie, G.; Yu, J.; Zhi, L. Facet-Mediated Photodegradation of Organic Dye over Hematite Architectures by Visible Light. *Angew. Chem., Int. Ed.* **2012**, *51*, 178.

- (17) Jiang, J.; Zhao, K.; Xiao, X. Y.; Zhnag, L. Z. Synthesis and Facet-Dependent Photoreactivity of BiOCl Single-Crystalline Nanosheets. *J. Am. Chem. Soc.* **2012**, *134*, 4473.
- (18) Wei, H.; Wang, E. K. Nanomaterials with Enzyme-like Characteristics (Nanozymes): Next-Generation Artificial Enzymes. *Chem. Soc. Rev.* **2013**, *42*, 6060.
- (19) Lin, Y.; Ren, J.; Qu, X. Nano-Gold as Artificial Enzymes: Hidden Talents. *Adv. Mater.* **2014**, *26*, 4200.
- (20) Lin, Y.; Ren, J.; Qu, X. Catalytically Active Nanomaterials: A Promising Candidate for Artificial Enzymes. *Acc. Chem. Res.* **2014**, *47*, 1097.
- (21) Liu, S.; Lu, F.; Xing, R.; Zhu, J.-J. Structural Effects of Fe_3O_4 Nanocrystals on Peroxidase-like Activity. *Chem.—Eur. J.* **2011**, *17*, 620.
- (22) Li, L.; Ai, L.; Zhang, C.; Jiang, J. Hierarchical {001}-Faceted BiOBr Microspheres as a Novel Biomimetic Catalyst: Dark Catalysis Towards Colorimetric Biosensing and Pollutant Degradation. *Nanoscale* **2014**, *6*, 4627.
- (23) Chaudhari, K. N.; Chaudhari, N. K.; Yu, J.-S. Peroxidase Mimic Activity of Hematite Iron Oxides ($\alpha\text{-Fe}_2\text{O}_3$) with Different Nanostructures. *Catal. Sci. Technol.* **2012**, *2*, 119.
- (24) Mitro, N.; Mak, P.; Vargas, L.; Godio, C.; Hampton, E.; Molteni, V.; Kresuch, A.; Saez, E. The Nuclear Receptor LXR Is a Glucose Sensor. *Nature* **2007**, *445*, 219.
- (25) Heller, A.; Feldman, B. Electrochemical Glucose Sensors and Their Applications in Diabetes Management. *Chem. Rev.* **2008**, *108*, 2482.
- (26) Zhou, Y.-X.; Yao, H.-B.; Zhang, Q.; Gong, J.-Y.; Liu, S.-J.; Yu, S.-H. Hierarchical FeWO_4 Microcrystals: Solvothermal Synthesis and Their Photocatalytic and Magnetic Properties. *Inorg. Chem.* **2009**, *48*, 1082.
- (27) Peng, Y.; Yan, M.; Chen, Q.-G.; Fan, C.-M.; Zhou, H.-Y.; Xu, A.-W. Novel One-Dimensional Bi_2O_3 – Bi_2WO_6 p–n Hierarchical Heterojunction with Enhanced Photocatalytic Activity. *J. Mater. Chem. A* **2014**, *2*, 8517.
- (28) Ai, L.; Jiang, J. Hierarchical Porous Quaternary Cu–Fe–Sn–S Hollow Chain Microspheres: Rapid Microwave Nonaqueous Synthesis, Growth Mechanism, and Their Efficient Removal of Organic Dye Pollutant in Water. *J. Mater. Chem.* **2012**, *22*, 20586.
- (29) Sun, X.; Guo, S.; Chung, C.-S.; Zhu, W.; Sun, S. A Sensitive H_2O_2 Assay Based on Dumbbell-like PtPd- Fe_3O_4 Nanoparticles. *Adv. Mater.* **2013**, *25*, 132.
- (30) Ai, L.; Li, L.; Zhang, C.; Fu, J.; Jiang, J. MIL-53(Fe): A Metal–Organic Framework with Intrinsic Peroxidase-like Catalytic Activity for Colorimetric Biosensing. *Chem.—Eur. J.* **2013**, *19*, 15105.
- (31) Wu, X.-Q.; Xu, Y.; Chen, Y.-L.; Zhao, H.; Cui, H.-J.; Shen, J.-S.; Zhang, H.-W. Peroxidase-like Activity of Ferrie Ions and Their Application to Cysteine Detection. *RSC Adv.* **2014**, *4*, 64438.
- (32) Wang, H.; Jiang, H.; Wang, S.; Shi, W.; He, J.; Liu, H.; Huang, Y. Fe_3O_4 -MWCNT Magnetic Nanocomposites as Efficient Peroxidase Mimic Catalysts in a Fenton-like Reaction for Water Purification without pH Limitation. *RSC Adv.* **2014**, *4*, 45809.
- (33) Zhang, Y.; Tian, J.; Liu, S.; Wang, L.; Qin, X.; Lu, W.; Chang, G.; Luo, Y.; Asiri, A. M.; Al-Youbicd, A. O.; Sun, X. Novel Application of CoFe Layered Double Hydroxides Nanoplates for Colorimetric Detection of H_2O_2 and Glucose. *Analyst* **2012**, *137*, 1325.
- (34) Liu, Y. L.; Zhao, X. J.; Yang, X. X.; Li, Y. F. A Nanosized Metal–Organic Framework of Fe-MIL-88NH₂ as A Novel Peroxidase Mimic Used for Colorimetric Detection of Glucose. *Analyst* **2013**, *138*, 4526.
- (35) Zhang, J.-W.; Zhang, H.-T.; Du, Z.-Y.; Wang, X.; Yu, S.-H.; Jiang, H.-L. Water-Stable Metal–Organic Frameworks with Intrinsic Peroxidase-like Catalytic Activity as a Colorimetric Biosensing Platform. *Chem. Commun.* **2014**, *50*, 1092.
- (36) Liu, S.; Tian, J.; Wang, L.; Luo, Y.; Chang, G.; Sun, X. Iron-Substituted SBA-15 Microparticles: A Peroxidase-like Catalyst for H_2O_2 Detection. *Analyst* **2011**, *136*, 4894.
- (37) Gao, L. Z.; Zhuang, J.; Nie, L.; Zhang, J. B.; Zhang, Y.; Gu, N.; Wang, T. H.; Feng, J.; Yang, D. L.; Perrett, S.; Yan, X. Y. Intrinsic Peroxidase-like Activity of Ferromagnetic Nanoparticles. *Nat. Nanotechnol.* **2007**, *2*, 577.
- (38) Chen, Y.; Cao, H.; Shi, W.; Liu, H.; Huang, Y. Fe-Co Bimetallic Alloy Nanoparticles as a Highly Active Peroxidase Mimetic and Its Application in Biosensing. *Chem. Commun.* **2013**, *49*, 5013.
- (39) Chen, Q.; Liu, M.; Zhao, J.; Peng, X.; Chen, X.; Mi, N.; Yin, B.; Li, H.; Zhang, Y.; Yao, S. Water-Dispersible Silicon Dots as a Peroxidase Mimetic for the Highly-Sensitive Colorimetric Detection of Glucose. *Chem. Commun.* **2014**, *50*, 6771.